Published in final edited form as:
Neuroscience. 2011 March 31; 178: 240–249. doi:10.1016/j.neuroscience.2011.01.023.

NMDA RECEPTOR SUBUNIT COMPOSITION IN THE RAT TRIGEMINAL PRINCIPAL NUCLEUS REMAINS CONSTANT DURING POSTNATAL DEVELOPMENT AND FOLLOWING NEONATAL DENERVATION

F.-S. LO[*] and **S. ZHAO**
Department of Anatomy and Neurobiology, University of Maryland School of Medicine, 20 Penn Street, Baltimore, Maryland, 21201, USA

Abstract

N-Methyl-D-Aspartate receptors (NMDARs) play a major role in various forms of developmental and adult synaptic plasticity (Lopez de Armentia and Sah 2003). Activity-dependent shifts in NR2 subunits of the NMDARs have been proposed to be the molecular basis of critical period plasticity. Several supporting examples have been reported; however it is not clear whether the relationship between NMDAR subunit changes and neural plasticity are correlative or causal, nor whether such a relationship is universal across all sensory pathways with developmental plasticity. In the present study, we used voltage-clamp recording techniques to investigate whether subunit composition of NMDARs changes during development and after neonatal denervation in the principal sensory nucleus (PrV) of the trigeminal nerve. Relative AMPA receptor contribution to synaptic transmission increased linearly by the second postnatal week in the normal PrV. Denervation by peripheral nerve damage did not alter this process. We took the weighted decay time constant (τ_w) of NMDAR-mediated EPSCs as an index for NMDAR subunit composition. The τ_w measurement and Western blot analysis revealed that NMDARs contained both NR2A and NR2B subunits. The NR2A/NR2B ratio did not change during postnatal development or after neonatal denervation. Thus, critical period plasticity-related pattern formation in the PrV does not depend on changes in subunit composition of NMDARs. The mechanism underlying developmental synaptic plasticity in the PrV differs from those in higher trigeminal centers and other brain structures.

Keywords

trigeminal brainstem; infraorbital nerve; glutamate receptors; NR2A subunit; NR2B subunit; synaptic plasticity

N-Methyl-D-Aspartate receptors (NMDARs) are heteromeric complexes, composed of the essential NR1 subunit and one or more NR2A-D subunits. The 2A and 2B subunits modulate kinetic properties of NMDA channels, allowing for faster or slower decay of

[*]Corresponding author: Dr. Fu-Sun Lo, Dept. Anatomy and Neurobiology, UMB SOM 20 Penn Street HSFII S220, Baltimore, MD, USA, Tel: +1-410-706-2130, Fax: +1-410-706-2512, Fusunlo@gmail.com.

excitatory postsynaptic currents (EPSCs) respectively (McBain and Mayer, 1994; Cull-Candy et al., 2001; Wenthold et al., 2003; Erreger et al., 2005). Thus, changes in expression patterns of these subunits might underlie various forms of developmental and adult synaptic plasticity (Quinlan et al., 1999b; Barth and Malenka, 2001; Cull-Candy et al., 2001; Lu et al., 2001; Townsend et al., 2003; Liu et al., 2004; Kopp et al., 2007; Yashiro and Philpot, 2008; Smith et al., 2009).

The rodent trigeminal pathway is an excellent model to study mechanisms of neural patterning and plasticity. In the brainstem trigeminal complex, presynaptic afferent arbors and postsynaptic target neurons form discrete modules ("barrelettes") that replicate the spatial distribution of whiskers and the sinus hairs on the snout. The trigeminal principal nucleus (PrV) is the first relay station along the trigeminal pathway, and conveys the whisker-specific patterns to the ventroposteromedial (VPM) nucleus of the thalamus and subsequently to the primary somatosensory cortex. Development and consolidation of the barrelettes depend on an intact sensory periphery during a critical period. Morphological studies illustrate that damage to the infraorbital (IO) nerve before postnatal day 4 (P4), whisker-specific patterning of trigeminal afferent arbors is lost and barrelette neurons reorient their dendritic trees from asymmetrical to nonspecific symmetric distribution (Belford and Killackey, 1980; Arends and Jacquin, 1993; Lo and Erzurumlu, 2001), suggesting reorganization of synaptic connections. Little is known about cellular mechanisms underlying patterning of neural connections and critical period plasticity in response to peripheral denervation during this period. Elecrophyiological studies show neonatal IO transection does not alter membrane properties of PrV neurons (Lo and Erzurumlu, 2001), but does change synaptic transmission in the PrV. Minimal stimulation of the trigeminal tract (TrV) reveals that synapses in the normal PrV are functional with AMPA and NMDA receptors at birth. After neonatal denervation, most functional synapses convert to silent synapses without functional AMPA receptors (Lo and Erzurumlu, 2007). Strong stimulation of the TrV induces a "plateau potential" that is mediated by L-type calcium channels and triggered by NMDAR-mediated EPSP in the denervated PrV (Lo and Erzurumlu, 2002). In recent years, genetic mutation studies in mice have revealed that two transcription factors and NMDARs are crucial for pattern formation in the PrV (see Erzurumlu et al., 2006; Erzurumlu and Iwasato, 2006, Erzurumlu et al., 2010 for reviews). In other brain structures, parallels between critical period plasticity and developmental shifts from the NMDAR subunits NR2B to NR2A have been shown (Carmignoto and Vicini, 1992; Scheetz and Constantine-Paton, 1994; Crair and Malenka, 1995; Quinlan et al., 1999b; Barth and Malenka, 2001; Cull-Candy et al., 2001; Erisir and Harris, 2003; Townsend et al., 2003). The question then arises whether critical period for synaptic plasticity in the PrV depends upon the change in NMDAR subunit.

EXPERIMENTAL PROCEDURES

Infraorbital nerve transection

Postnatal day 0 (P0) Sprague-Dawley rat pups were anesthetized by Fluothane (Halothane) inhalation and a unilateral skin incision was made caudal to the whisker pad. The infraorbital (IO) nerve was visualized and cut with sterile micro scissors. After the pups recovered from anesthesia, they were returned to their home cage. All animal handling was in accordance with the National Institute of Health Guide for the Care and Use of Laboratory Animals (NIH Publications No. 80-23) revised 1996 and a protocol approved by UMB Animal Use and Care Committee.

Brain slice preparation

Rat pups were deeply anesthetized with Fluothane and then euthanized by decapitation. The brain was removed and immersed in cold (4°C), sucrose-based artificial cerebrospinal fluid (ACSF, in mM: Sucrose, 234; KCl, 2.5; NaH_2PO_4, 1.25; $MgSO_4$, 10; $NaHCO_3$, 24; glucose, 11; $CaCl_2$, 0.5) bubbled with 95% O_2 and 5% CO_2 (pH=7.4). The brainstem was embedded in 2% agar and cut into 400 μm thick transverse sections with a vibratome (Electron Microscopy Sciences). Slices containing the PrV were placed in a submerged-type recording chamber (Fine Science Tools) and continuously perfused (2 ml/min) with normal ACSF (in mM: NaCl, 124; KCl, 2.5; NaH_2PO_4, 1.25; $MgSO_4$, 2; $NaHCO_3$, 26; glucose, 10; $CaCl_2$, 2, pH=7.4) at room temperature. During recording, bicuculline (10 μM) or picrotoxin (100 μM, Sigma, St. Louis, MO) was added to the ACSF to block GABAergic responses.

Electrophysiological methods

Recordings began at least 1 hour after incubation in normal ACSF. Whole-cell-patch micropipettes were pulled horizontally in four stages from borosilicate glass. The patch electrodes were backfilled with a cesium-based solution containing (in mM): $CsMeSO_3$, 115; NaCl, 10; KCl, 1; $MgCl_2$, 4; $CaCl_2$, 1, EGTA, 10; HEPES, 20; Na_2-ATP, 3; Na_3-GTP, 0.5; spermine, 0.1 (pH=7.25) ($CsMeSO_3$ and spermine were purchased from Sigma) with a tip resistance of 5–9 MΩ. Neurons in the ventral part of the PrV (barrelette region) were blindly patched (Lo et al., 1999). After “break-in”, the serial resistance was completely compensated with bridge balance of AxoClamp 2B amplifier. We only collected data from cells with resting membrane potential negative to −55 mV and input resistance >200 MΩ with an Instrutek ITC-16 interface unit and stored on a Pentium 4 computer with Pulses (HEKA) software program. Both current clamp and continuous voltage clamp were performed on recorded cells. Different DC pulse protocols were used to induce active conductances of PrV cells. Barrelette cells were identified by their A-type K^+ conductance, and interbarrelette cells, by T-type low threshold Ca^{2+} conductance (Lo et al., 1999).

A pair of fine-tip stimulating electrodes (0.5 MΩ, WPI, IRM33A05KT, tip diameter: 2–3 μm, separated by 300 μm) was inserted into the TrV lateral to the ventral PrV (barrelette region). We used a supra-threshold (5 times of threshold intensity) stimulus by passing current pulses (0.2–0.5 ms duration, <400 μA) through the electrodes at 0.33 Hz. Identification of AMPA- and NMDA- receptor-mediated EPSCs was based on their voltage dependency and their responses to glutamate antagonists. The AMPA receptor-mediated EPSC (AMPA-EPSC) was blocked by 1,2,3,4-tetrahydro-6-nitro-2,3-dioxo-benzo[f]quinoxaline-7-sulfonamide (NBQX, 10 μM) (Sigma) and increased in amplitude with membrane hyperpolarization. The NMDAR-mediated EPSC (NMDA-EPSC) was identified by its nonlinear voltage dependency in the presence of 2 mM Mg^{2+} and blockade by D(−)-2-amino-5-phosphono-pentanoic acid (D-APV, 100 μM, Sigma).

Data analysis

We first averaged 10 traces of EPSCs clamped at +60 mV or −70 mV. Based on the data from pharmacologically isolated AMPA- and NMDAR-EPSCs (described in Results), we measured the amplitudes of EPSCs (clamped at +60 mV) at 8 ms and 30 ms after TrV stimulation as AMPA-EPSC and NMDA-EPSC, to compute the AMPA/NMDA ratio, in a manner similar to that used by others (Laurent et al., 2002). The decay of NMDA-EPSC at +60 mV was fit with a double exponential formula:

$$I(t)=I_f \times \exp(-t/\tau_f)+I_s \times \exp(-t/\tau_s)$$

Where I_f and I_s are the amplitudes of the fast and slow decay components, and τ_f and τ_s are their respective decay time constants. Then, we calculated the weighted decay time constant:

$$\tau_w = I_f/(I_f+I_s) \times \tau_f + I_s/(I_f+I_s) \times \tau_s$$

(Vicini et al., 1998; Lu et al., 2001).

Data were expressed as mean ± S.E.M. A Student's *t*-test was used to determine statistical significance. Linear correlation and regression were performed with SigmaPlot software to show developmental changes in the AMPA/NMDA ratio and τ_w of NMDA-EPSCs. We used "Analysis of Covariance" (ANCOVA) to compare different linear regression lines. ANOVA (analysis of variance) was used to compare multiple data sets.

Western blot

For Western blot analyses, 6 litters of P0 unilateral IO-lesioned rat pups were euthanized on P5, and P14. The brains were extracted and sliced on a McIlwain tissue chopper at 700–1000 μm. Slices containing the PrV were selected under a stereomicroscope and the PrV was dissected out using microscissors. The left and right (lesioned side) PrV from each animal and age were collected in Eppendorf tubes and rapidly frozen. In all cases the whisker pad was dissected to ensure that the nerve cut was complete. 25 μg protein from each sample was separated on 7.5% SDS-PAGE gel (Bio-Rad), and electroblotted to nitrocellulose membrane (GE Healthcare). The membranes were incubated in blocking solution (5% milk in TRIS buffered saline with Tween20 (TBS-T) for 1 h at room temperature), then incubated with anti-rabbit NR2A (1:1000 Upstate) or NR2B (1:1000 Alomone Lab) with 5% milk in TBS-T overnight at 4 °C. Following 3 washes with TBS-T, the membranes were incubated for 1 h at room temperature in goat anti-rabbit IgG horseradish peroxidase (HRP) (1:5000 Bio-Rad) in 5% milk in TBS-T. After TBS-T washes the immunoreactivity was detected using Super Signal West pico chemiluminescent substrate (Thermo Scientific) for HRP. To monitor the loading and blotting of equal amount of protein, the membranes were incubated with an antibody against actin (1:500, Sigma-Aldrich). The ECL-exposed films were quantified by comparing the intensity of the bands on a western blot (Image J version 1, from the National Institutes of Health.) Five samples for each time point were tested. Intensity measurements were normalized to actin levels and averaged (mean ± S.E.M.). ANOVA was used to analyze Western blot results.

RESULTS

The PrV contains three classes of neurons. Barrelette neurons display a transient K^+ (I_A) conductance and receive monosynaptic excitatory and disynaptic inhibitory inputs upon stimulation of the trigeminal tract (TrV) (Lo et al., 1999). Interbarrelette neurons are distinguished by low-threshold T-type Ca^{2+} current (I_T) and receive excitatory inputs from multiple sources (Lo et al., 1999). Finally, GABAergic interneurons contribute to the intranuclear inhibitory circuitry (Lo et al., 1999). Here, we focused on excitatory (barrelette and interbarrelette) neurons.

Excitatory responses in developing barrelette and interbarrelette cells are mediated by both AMPA and NMDA receptors

We performed whole-cell recordings from barrelette and interbarrelette neurons in the PrV of postnatal rats on P0–P13. Immediately after the formation of whole-cell configuration, we first tested the active conductances of recorded neurons. Current clamp recordings with Cs^+-containing electrodes showed that barrelette cells exhibited an A-type K^+ conductance (I_A) (Fig. 1A) that was gradually blocked by Cs^+ dialyzed from patch electrode about 3 min later.

Interbarrelette cells showed a T-type low threshold Ca^{2+} conductance (I_T) (Fig. 1B). Then, we performed voltage-clamp recordings to investigate the excitatory postsynaptic current (EPSC) evoked by supra-threshold stimulation of the trigeminal tract (TrV) in the presence of GABAergic antagonists. The EPSC that was clamped at +60 mV consisted of two components in both barrelette (Fig. 1C upper traces) and interbarrelette (Fig. 1D upper traces) cells. The early component declined rapidly and the late component declined slowly. In the ACSF containing 2 mM Mg^{2+}, the late component of the EPSC was much smaller in amplitude but not completely abolished at −70 mV as compared with that at +60 mV (Fig. 1C and D lower vs. upper traces). These results suggest that the early component of the EPSC is mediated by AMPA receptors that contain the GluR2 subunit because its amplitude does not decrease at positive membrane potentials, and thus lacks inward rectification (Verdoorn et al., 1991).

Application of NBQX (10 μM), an AMPA antagonist, blocked the early component, thus disclosing a late NMDAR-mediated EPSC (NMDA-EPSC) in both cell types (Fig. 1E and F, *1*, before, *2*, after application). In order to investigate the function of NMDARs under physiological condition, we also applied AMPA antagonist NBQX to get pure NMDA-EPSCs at −70 mV (Fig. 1F). In the presence of 2 mM Mg^{2+}, a considerable amount of NMDA-EPSC remained (Fig 1F, interbarrelette cell; also see Fig. 1, C and D lower traces), suggesting that NMDARs still play a role in synaptic transmission at resting membrane potential. As shown in Fig 1E and F, the NMDA-EPSC mainly contributed to the late component of the EPSC in both barrelette and interbarrelette neurons. Application of D-APV (100 μM), an NMDA antagonist, blocked the late component and left the early AMPAR-mediated EPSC (AMPA-EPSC) intact in both cell types (Fig. 1G and H, *1* vs. *2*). Excitatory postsynaptic responses in barrelette and interbarrelette cells in the PrV were mediated by both AMPA and NMDA receptors at all ages studied (P0–P13). This result supports previous reports that synapses in the PrV are already functional at birth (Waite et al., 2000; Lo and Erzurumlu, 2007).

Developmental changes in AMPA/NMDA ratio of EPSCs

We quantitatively analyzed pharmacologically isolated AMPA-EPSCs and NMDA-EPSCs at a holding potential of +60 mV. The latency to the AMPA-EPSC peak amplitude was ~8 ms (8.3 ± 0.7 ms, n=7). The latency to the NMDA-EPSC peak amplitude was ~30 ms (29 ± 2.5 ms, n=7). In Fig. 1I and J, we superimposed pharmacologically isolated AMPA-EPSC and calculated D-APV sensitive NMDA-EPSC from each cell. Note that the expanded traces in insets show that AMPA- and NMDA-EPSCs slightly overlap. When the AMPA-EPSC reached its peak, the overlapped NMDA-EPSC had only risen to 9 ± 3 % (n=7) of its peak value. When the NMDA-EPSC reached its peak, the amplitude of the AMPA-EPSC had dropped to 7±1% (n=7) of its peak value. Based on these measurements, we selected two time points (8 ms and 30 ms) to determine the AMPA/NMDA ratio of the compound EPSCs in the absence of glutamate antagonists. Though not as accurate as pharmacological isolation of different components, this timing measurement is a suitable way to determine AMPA/NMDA ratio without pharmacology (Laurent et al., 2002). An example of I-V curves plotted from 10 neurons is presented in Fig. 2A. The amplitude at 8 ms exhibited a linear I-V curve that fits AMPA receptor properties, while the amplitude at 30 ms showed a non-linear I-V curve, a typical voltage-dependence of NMDA responses in the presence of 2 mM Mg^{2+}.

We calculated the AMPA/NMDA ratio of barrelette and interbarrelette neurons separately and plotted the AMPA/NMDA ratio against postnatal ages. In the normal PrV, the AMPA/NMDA ratio of barrelette neurons (n=24) increased along with postnatal development. There was a linear correlation ($R=0.64$, $p<0.001$) between the AMPA/NMDA ratio and postnatal ages (Fig. 2D, closed circles and dashed line). In the normal interbarrelette neurons (n=30), the AMPA/NMDA ratio also increased developmentally. There was a linear

correlation (R=0.63, p<0.001) between the AMPA/NMDA ratio and postnatal ages (Fig. 2E, closed circles and dashed line). Analysis of covariance (ANCOVA) showed no difference in the slopes and intercepts of linear regression lines between the two cell types (p=0.92). Thus, the AMPA/NMDA ratio is developmentally enhanced in both barrelette and interbarrelette neurons of the normal PrV. The change in the AMPA/NMDA ratio does not coincide with critical period plasticity, and occurs similarly in both barrelette and interbarrelette cells (see sample records showing the developmental increase in the AMPA/NMDA ratio in Fig. 2B (upper vs. lower traces)).

Neonatal denervation does not alter the developmental increase in the AMPA/NMDA ratio of EPSCs

In the denervated PrV, barrelette and interbarrelette cells are also distinguished by A-type K^+ and T-type Ca^{2+} conductance respectively (Lo and Erzurumlu, 2001). Although minimal stimulation of the TrV induced only NMDA-EPSCs without AMPA-EPSCs in the denervated PrV (Lo and Erzurumlu, 2007), supra-thrshold stimulation evoked both AMPA- and NMDA-EPSCs. In the denervated barrelette neurons (n=24), there was a weaker linear correlation between the AMPA/NMDA ratio and postnatal ages (R=0.51, p<0.01, Fig. 2D, open circles, dotted line). Analysis of covariance (ANCOVA) showed no difference in the slopes and intercepts of linear regression lines between normal and denervated barrelette neurons (p=1.00). The AMPA/NMDA ratio of denervated interbarrelette neurons (n=26) was also linearly correlated with the postnatal ages (R=0.63, p<0.001, Fig. 2E, open circles, dotted line). Analysis of covariance showed the slopes and intercepts of regression lines was similar between normal and denervated interbarrelette neurons (p=0.58). In addition, the slopes and intercepts of regression lines were similar to those for normal barrelette and interbarrelette neurons (p=0.61). Sample records showing the developmental increase in the AMPA/NMDA ratio are presented in Fig. 2C (upper vs. lower traces). We conclude that neonatal denervation does not alter the developmental increase in the AMPA/NMDA ratio, which is apparently independent of sensory activity from whiskers.

The weighted time constant (τ_w) of NMDA-EPSC decay in the PrV remains constant during postnatal development

Since the shift of NMDA subunits is thought to provide a molecular basis for critical period plasticity (Carmignoto and Vicini, 1992; Scheetz and Constantine-Paton, 1994; Crair and Malenka, 1995; Erisir and Harris, 2003), we examined whether NMDAR subunit composition is altered during postnatal development. The weighted time constant (τ_w) of NMDA-EPSC decay has been used to delineate NMDA subunit composition (Vicini et al., 1998). We measured and calculated τ_w values in normal barrelette and interbarrelette neurons, and plotted τ_w against postnatal ages for each cell type. In normal barrelette neurons (n=18), there was no linear correlation between τ_w values and postnatal ages (R=0.18, p>0.45), nor could fit the data with nonlinear correlation (Fig. 3A, Normal Barrelette). Thus, the τ_w values are not developmentally regulated. Similarly, the τ_w values of normal interbarrelette neurons (n=17) were not linearly (R=0.23, p>0.36) or exponentially correlated with postnatal ages (Fig. 3A, Normal Interbarrelette).

To compare the τ_w values between the two cell types, we arbitrarily divided data into the first postnatal week (P0–6) and the second postnatal week (P7–13). The mean τ_w of normal barrelette neurons was 287±53 ms (n=11) in the first postnatal week and 260±69 ms (n=7) in the second week. There was no significant difference (p>0.77) between the two weeks (Fig. 3B, Black and white bars labeled “Normal Barrelette”). The mean τ_w of normal interbarrelette neurons was 259±549 ms (n=11) in the first postnatal week and 257±71 ms (n=6) in the second week. The τ_w values of both weeks were about the same (p>0.98, Fig. 3B, black and white bars labeled “Normal Interbarrelette”). The τ_w values were not

significantly different between barrelette and interbarrelette neurons (p>0.72). These results suggest that subunit composition of NMDARs of both cell types remains constant during postnatal development.

Neonatal denervation does not alter the weighted time constant (τ_w) of NMDA-EPSC decay

In the denervated PrV, the τ_w values were not linearly correlated with postnatal ages in either barrelette (R=0.17, p>0.49, Fig. 3A, IO Cut Barrelette) or interbarrelette neurons (R=0.25, p>0.35, Fig. 3A, IO Cut Interbarrelette), nor could we fit the data with nonlinear correlation. The mean τ_w for denervated barrelette cells was 241±44 ms (n=11) in the first postnatal week and 254±32 ms (n=8) in the second week (Fig. 3B, bars labeled "IO Cut Barrelette"). There was no developmental change (p>0.84) in the τ_w values of denervated barrelette neurons. The mean τ_w for denervated interbarrelette cells was 281±75 ms (n=12) in the first postnatal week and 225±47 ms (n=5). There was no significant difference (p>0.67) between them (Fig. 3B, bars labeled "IO Cut Interbarrelette"). The τ_w values for both cell types were similar (p>0.64). Therefore, neonatal denervation did not affect the similarity in the τ_w value of NMDA-EPSCs between barrelette and interbarrelette cells. Then, we compared the τ_w values obtained from denervated PrV with those from normal PrV. ANOVA analysis showed no significant differences were found between them (p>0.99). Collectively, these results suggest that denervation does not alter subunit composition of NMDAR in either barrelette or interbarrelette neurons of the PrV.

NMDARs contain both NR2A and NR2B subunits during postnatal development and after denervation

The value of τ_w suggests that NMDARs contain the NR2B subunit (Vicini et al., 1998; Cull-Candy et al., 2001). We applied α-[4-hydroxyphenyl-]-β-methyl-4-benzyl-1-piperidine-ethanol (ifenprodil, 3 μM), an NR2B-specific antagonist (Williams, 1993) to barrelette (n=4) and interbarrelette neurons (n=3). EPSCs at +60 mV of barrelette and interbarrelette neurons were partially blocked by ifenprodil. On average, ifenprodil induced a 77.4% reduction in τ_w values (data not shown), suggesting that NMDARs in the PrV contain both NR2A and NR2B subunits. We used Western blot analysis to test NR2A and NR2B protein expression. The Western blots suggest that the NR2A and NR2B proteins remain constant during postnatal development and after neonatal denervation. Both NR2A and NR2B protein was present (Fig. 4A) in the first and second postnatal weeks. The intensity measurements of NR2A and NR2B were normalized to actin levels and expressed as relative intensity. In the normal PrV (control), NR2A and NR2B expressions were about the same at P5 and P14 (Fig. 4B) suggesting that there is no developmental change in NR2A and NR2B levels. ANOVA showed no significant difference (n=5, p=0.97) between NR2A and NR2B expression, indicating the NR2A/NR2B ratio is around 1. We compared NR2A expression between normal side and IO Cut side at various ages (Fig. 4C). ANOVA also showed no significant difference (n=5, p=0.75) between the sides, suggesting that neonatal denervation does not change NR2A subunit expression. We compared NR2B expression on both sides at different postnatal ages (Fig. 4D). ANOVA revealed p=0.97, indicating that NR2B expression is not affected by neonatal denervation.

DISCUSSION

NMDAR-mediated activity plays a major role in development of whisker-specific barrelette patterns in the PrV, the first relay station of the trigeminal somatosensory pathway. Studies using gene knockout technology in mice showed that in the absence of either NR1 or NR2B subunits, or in NR1 knockdown mice, barrelettes do not form (Kutsuwada et al., 1996; Iwasato et al., 1997; Li. et al., 1994; Lee et al., 2005). A developmental decrease in the duration of NMDA-EPSCs has been observed in several brain structures including

trigeminal higher centers (the thalamic VPM and barrel cortex) (Carmignoto and Vicini, 1992; Hestrin, 1992; Crair and Malenka, 1995; Flint et al., 1997; Hsia et al., 1998; Roberts and Ramoa, 1999; Rumbaugh and Vicini, 1999; Lu et al., 2001; Steinert et al., 2010). The shortening of NMDA-EPSCs is a consequence of shifts from the NMDAR subunits NR2B to NR2A (Scheetz and Constantine-Paton, 1994; Crair and Malenka, 1995; Flint et al., 1997; Quinlan et al., 1999a; 1999b; Roberts and Ramoa, 1999; Sans et al., 2000; Barth and Malenka, 2001; Cull-Candy et al., 2001; Turman et al., 2002; Erisir and Harris, 2003; Townsend et al., 2003; Liu et al., 2004; Zundert et al., 2004; Xing et al., 2006). This developmental shift from NR2B to NR2A subunits depends on sensory experience, because deprivation of sensory inputs during critical period delays it or prolongs the NR2B subunit expression (Carmignoto and Vicini, 1992; Quinlan et al., 1999b; Philpot et al., 2001; Mierau et al., 2004).

Since the shift of NMDA subunits is roughly in parallel with the reduction in synaptic plasticity, it has been proposed to be the molecular basis for critical period plasticity (Carmignoto and Vicini, 1992; Scheetz and Constantine-Paton, 1994; Crair and Malenka, 1995; Erisir and Harris, 2003; Corson et al., 2009). Our present results rule out such a scenario for critical period plasticity in the PrV. The weighted time constant (τ_w) of NMDA-EPSC decay is around 250 ms and remains unchanged during postnatal development. Western blot analyses show no developmental changes in NR2A and NR2B protein expression. The data indicate that subunit composition of NMDARs is constant during the first two postnatal weeks, suggesting that the mechanism underlying critical period plasticity in the PrV differs from those in other brain structures. Likewise, the dorsal horn of the spinal cord and some subdivisions of vestibular nucleus and amygdala fail to exhibit a developmental decrease in NR2B subunit expression (Sans et al., 1997; Sans et al., 2000; Brown et al., 2002; Karlsson et al., 2002; Lopez de Armentia and Sah, 2003; Tse et al., 2008; Lai et al., 2008), suggesting that this subunit shift is far from a universal mechanism.

Our results illustrate that in the PrV of rats, the AMPA/NMDA ratio increases with postnatal development, and is unaltered by neonatal denervation. A developmental increase in AMPA/NMDA ratio has been reported in other brain structures (Crair and Malenka, 1995; Hsia et al., 1998; Mierau et al., 2004; Ye et al., 2005). In the PrV of rats, the increase in AMPA/NMDA ratio is neither correlated with critical period plasticity nor dependent on sensory activity from whiskers. Thus, it might be activity-independent, or dependent on spontaneous activity of trigeminal ganglion cells (Chudler and Anderson, 2002). Spontaneous firing rate of trigeminal ganglion cells is relatively low (<10 Hz) (Minnery and Simons, 2003; Shoykhet et al., 2003), but might play a role in the development of synaptic transmission.

NR2B-containing NMDA receptors are associated with synaptic plasticity, learning and memory, chronic pain and various neurological diseases (see Mony et al., 2009; Yashiro and Philpot, 2008; Zhou, 2009 for reviews). What is the functional significance of the constancy of the NR2B subunits in the PrV? We know that the majority of trigeminal ganglion cells and PrV neurons show slowly adapting responses. They display tonic discharges in the "plateau phase" of whisker deflection (Minnery and Simons, 2003). Thus, NR2B-containing NMDARs may contribute to synaptic transmission of tonic afferent impulses. As we demonstrated before (Lo et al., 1999), PrV neurons receive disynaptic IPSPs. Repetitive afferent impulses induce temporal summation of IPSPs that curtail tonic firing in postsynaptic neurons. However, NR2B-containing NMDAR-mediated EPSPs have a long duration. Repetitive inputs result in temporal summation of these EPSPs that facilitate tonic firing. Therefore, the balance of EPSPs and IPSPs ensures faithful transmission of tonic firing from trigeminal ganglion cells to PrV neurons (Minnery and Simons, 2003). In sharp contrast, fewer neurons exhibit slowly adapting responses upon whisker deflection and their tonic discharges are at lower frequency in the ventroposteromedial nucleus (VPM) and

barrel cortex, (Simons and Carvell, 1989; Hartings et al., 2000). The attenuation of tonic responses results from thalamic inhibition that suppresses tonic activity (Hartings and Simons, 2000). However, PrV cells also receive inhibitory inputs (Lo et al., 1999), but still display tonic discharges upon whisker deflection. The difference in the expression of the NR2B subunits may account for this discrepancy. The PrV always shows high expression of the NR2B subunits, while the VPM and barrel cortex lack the NR2B subunits after critical period (Lu et al., 2001; Liu et al., 2004; Mierau et al., 2004). Thus, NR2B subunit-containing NMDARs might be required for tonic responses in the trigeminal pathway. It would be interesting to examine whether neurons with tonic responses in other systems also have NR2B-containing NMDARs.

Acknowledgments

We thank Dr. R. S. Erzurumlu for his financial support and valuable help and Dr. A. Yang for advice and support with protein analysis. We are also indebted to Drs. L.-J. Lee and S. Chebabo-Weiner for their efforts on immunohistochemistry. This work was supported by NIH Grant NS037070.

Abbreviations

AMPA receptor	α-amino-3-hydroxy-5-methyl-4-isoxazolepropionic acid receptor
ANCOVA	analysis of Covariance
ANOVA	analysis of variance
D-APV	D(−)-2-Amino-5-phosphono-pentanoic acid
EPSC	excitatory postsynaptic current
IO	the infraorbital nerve
NBQX	1,2,3,4-Tetrahydro-6-nitro-2,3-dioxo-benzo[f]quinoxaline-7-sulfonamide
NMDARs	N-Methyl-D-Aspartate receptors
Pn	postnatal day n
PrV	the trigeminal principal nucleus
TrV	the trigeminal tract
τ_w	the weighted decay time constant
VPM	thalamic ventroposteromedial nucleus

REFEREENCES

Arends JJA, Jacquin MF. Lucifer yellow staining in fixed brain slices: optimal methods and compatibility with somatotopic markers in neonatal brain. J Neurosci Meth 1993;50:321–339.

Barth AL, Malenka RC. NMDAR EPSC kinetics do not regulate the critical period for LTP at thalamocortical synapses. Nat Neurosci 2001;4:235–236. [PubMed: 11224537]

Belford GR, Killackey HP. The sensitive period in the development of the trigeminal system of the neonatal rat. J Comp Neurol 1980;193:335–350. [PubMed: 7440771]

Brown KM, Wrathall JR, Yasuda RP, Wolfe BB. Quantitative measurement of glutamate receptor subunit protein expression in the postnatal spinal cord. Dev Brain Res 2002;137:127–133. [PubMed: 12220704]

Carmignoto G, Vicini S. Activity-dependent decrease in NMDA receptor responses during development of the visual cortex. Science 1992;258:1007–1011. [PubMed: 1279803]

Chudler EH, Anderson LC. Behavioral and electrophysiological consequences of deafferentation following chronic constriction of the infraorbital nerve in adult rats. Arch Oral Biol 2002;47:165–172. [PubMed: 11825581]

Corson J, Nahmani M, Lubarsky K, Badr N, Wright C, Erisir A. Sensory activity modulates N-methyl-D-aspartate receptor subunits 2A and 2B in cortical layers. Neuroscience 2009;163:920–932. [PubMed: 19596055]

Crair MC, Malenka RC. A critical period for long-term potentiation at thalamocortical synapses. Nature 1995;375:325–328. [PubMed: 7753197]

Cull-Candy S, Brickley S, Farrant M. NMDA receptor subunits: diversity, development and disease. Curr Opin Neurobiol 2001;11:327–335. [PubMed: 11399431]

Erisir A, Harris JL. Decline of the critical period of visual plasticity is concurrent with the reduction of NR2B subunit of the synaptic NMDA receptor in layer 4. J Neurosci 2003;23:5208–5218. [PubMed: 12832545]

Erreger K, Dravid SM, Banke TG, Wyllie DJA, Traynelis SF. Subunit-specific gating controls rat NR1/NR2A and NR1/NR2B NMDA channel kinetics and synaptic signaling profiles. J Physiol 2005;563.2:345–358. [PubMed: 15649985]

Erzurumlu, RS.; Iwasato, T. Patterning of the somatosensory maps with NMDA receptors. In: Erzurumlu, RS.; Guido, W.; Molnar, Z., editors. Development and Plasticity in Sensory Thalamus and Cortex. Springer; 2006. p. 158-182.

Erzurumlu RS, Chen ZF, Jacquin MF. Molecular determinants of the face map development in the trigeminal brainstem. Anat Rec A Discov Mol Cell Evol Biol 2006;288:121–134. [PubMed: 16432893]

Erzurumlu RS, Murakami Y, Rijli FM. Mapping the face in the somatosensory system. Nature Reviews 2010;11:252–263.

Flint AC, Maisch US, Weishaupt JH, Kriegstein AR, Monyer H. NR2A subunit expression shortens NMDA receptor synaptic currents in developing neocortex. J Neurosci 1997;17:2469–2476. [PubMed: 9065507]

Hartings JA, Simons DJ. Inhibition suppresses transmission of tonic vibrassa-evoked activity in the rat ventrobasal thalamus. J Neurosci 2000;20(RC100):1–5. [PubMed: 10627575]

Hartings JA, Temereanca S, Simons DJ. High responsiveness and direction sensitivity of neurons in the rat thalamic reticular nucleus to vibrissa deflections. J Neurophysiol 2000;83:2791–2801. [PubMed: 10805677]

Hestrin S. Developmental regulation of NMDA receptor-mediated synaptic currents at a central synapse. Nature 1992;375:686–689. [PubMed: 1377360]

Hsia AY, Malenka RC, Nicoll RA. Development of excitatory circuitry in the hippocampus. J Neurophysiol 1998;79:2013–2024. [PubMed: 9535965]

Iwasato T, Erzurumlu RS, Huerto PT, Sasaoka T, Ulupinar E, Tonegawa S. NMDA receptor-dependent refinement of somatotopic maps. Neuron 1997;19:1–20. [PubMed: 9247258]

Karlsson U, Sjodin J, Moller KA, Johansson S, Wiksrom L, Nasstrom J. Glutamate-induced current reveal three functionally distinct NMDA receptor populations in rat dorsal horn-effects of peripheral nerve lesson and inflammation. Neuroscience 2002;112:861–868. [PubMed: 12088745]

Kopp C, Longordo F, Lüthi A. Experience-dependent changes in NMDA receptor composition at mature central synapses. Neuropharm 2007;53:1–9.

Kutsuwada T, Sakimura K, Manabe T, Takayama C, Katakura N, Kushiya E, Natsume R, Watanabe M, Inoue Y, Yagi T, Aizawa S, Arakawa M, Takahashi T, Nakamura Y, Mori H, Mishina M. Impairment of sucking response, trigeminal neuronal pattern formation, and hippocampal LTD in NMDA receptor e2 subunit mutant mice. Neuron 1996;16:333–344. [PubMed: 8789948]

Lai S-K, Lai C-H, Tse Y-C, Yung KKL, Shum DKY, Chan Y-S. Developmental maturation of ionotropic glutamate receptors subunits in rat vestibular nuclear neurons responsive to vertical linear acceleration. Eur J Neurosci 2008;28:2157–2172. [PubMed: 19046363]

Laurent A, Goaillard J-M, Cases O, Lebrand C, Gaspar P, Ropert N. Activity-dependent presynaptic effect of serotonin 1B receptors on the somatosensory thalamocortical transmission I neonatal mice. J Neurosci 2002;22:886–900. [PubMed: 11826118]

Lee L-J, Lo F-S, Erzurumlu RS. NMDA receptor-dependent regulation of axonal and dendritic branching. J Neurosci 2005;25:2304–2311. [PubMed: 15745956]

Li Y, Erzurumlu RS, Chen C, Jhaveri S, Tonegawa S. Whisker-related neuronal patterns fail to develop in the brainstem trigeminal nuclei of NMDAR1 knockout mice. Cell 1994;76:427–437. [PubMed: 8313466]

Liu X-B, Murray KD, Jones EG. Switching of NMDA receptor 2A and 2B subunits at thalamic and cortical synapses during early postnatal development. J Neurosci 2004;24:8885–8895. [PubMed: 15470155]

Lo F-S, Erzurumlu RS. Neonatal deafferentation does not alter membrane properties of trigeminal nucleus principalis neurons. J Neurophysiol 2001;85:1088–1096. [PubMed: 11247979]

Lo F-S, Erzurumlu RS. L-type calcium channel-mediated plateau potentials in barrelette cells during structural plasticity. J Neurophysiol 2002;88:794–801. [PubMed: 12163531]

Lo F-S, Erzurumlu RS. Conversion of functional synapses into silent synapses in the trigeminal brainstem after neonatal peripheral nerve transection. J Neurosci 2007;27:4929–4934. [PubMed: 17475801]

Lo F-S, Guido W, Erzurumlu RS. Electrophysiological properties and synaptic responses of cells in the trigeminal principal sensory nucleus of postnatal rats. J Neurophysiol 1999;82:2765–2775. [PubMed: 10561443]

Lopez de Armentia M, Sah P. Development and subunit composition of synaptic NMDA receptors in the amygdala: NR2B synapses in the adult central amygdala. J Neurosci 2003;23:6876–6883. [PubMed: 12890782]

Lu H-C, Gonzales E, Crair MC. Barrel cortex critical period plasticity is independent of changes in NMDA receptor subunit composition. Neuron 2001;32:619–634. [PubMed: 11719203]

McBain CJ, Mayer ML. N-methyl-D-aspartic acid receptor structure and function. Physiol Rev 1994;74:723–760. [PubMed: 8036251]

Mierau SB, Meredith RM, Upton AL, Paulsen O. Dissociation of experience-dependent and -independent changes in excitatory synaptic transmission during development of barrel cortex. Proc Natl Acad Sci USA 2004;101:15518–15523. [PubMed: 15492224]

Minnery BS, Simons DJ. Response properties of whisker-associated trigeminothalamic neurons in rat nucleus principalis. J Neurophysiol 2003;89:40–56. [PubMed: 12522158]

Mony L, Kew JNC, Gunthorpe MJ, Paoletti P. Allosteriic modulator of NR2B-containing NMDA receptors: moleculr mechanisms and therapeautic potential. Br J Pharmacol 2009;157:1301–1317. [PubMed: 19594762]

Philpot BD, Sekhar AK, Shouval HZ, Bear MF. Visual experience and deprivation bidirectionally modify the composition and function of NMDA receptors in visual cortex. Neuron 2001;29:157–169. [PubMed: 11182088]

Quinlan EM, Olstein DH, Bear MF. Bidirectional, experience-dependent regulation of N-methyl-D-aspartate receptor subunit composition in the rat visual cortex during postnatal development. Proc Natl Acad Sci USA 1999a;96:12876–1288. [PubMed: 10536016]

Quinlan EM, Philpot BD, Huganir RL, Bear MF. Rapid, experience-dependent expression of synaptic MDA receptors in visual cortex in vivo. Nat Neurosci 1999b;2:352–357. [PubMed: 10204542]

Roberts EB, Ramoa AS. Enhanced NR2A subunit expression and decreased NMDA receptor decay time at the onset of ocular dominance plasticity in the ferret. J Neurophysiol 1999;81:2587–2591. [PubMed: 10322092]

Rumbaugh G, Vicini S. Distinct synaptic and extrasynaptic NMDA receptors in developing cerebellar granule neurons. J Neurosci 1999;19:10603–10610. [PubMed: 10594044]

Sans N, Petralia S, Wang Y-X, Blahos J II, Hell JW, Wenthold RJ. A developmental change in NMDA receptor-associated proteins at hippocampal synapses. J Neurosci 2000;20:1260–1271. [PubMed: 10648730]

Sans N, Sans A, Raymond J. Regulation of NMDA receptor subunit mRNA expression in the guinea pig vestibular nuclei following unilateral labyrinthectomy. Eur J Neurosci 1997;9:2019–2034. [PubMed: 9421163]

Scheetz AJ, Constantine-Paton M. Modulation of NMDA receptor function: implications for vertebrate neural development. FASEB J 1994;8:745–752. [PubMed: 8050674]

Shoykhet M, Shetty P, Minnery BS, Simons DJ. Protracted development of responses to whisker deflection in rat trigeminal ganglion neurons. J Neurophysiol 2003;90:1432–1437. [PubMed: 12801899]

Smith GB, Heynen AJ, Bear MF. Bidirectional synaptic mechanisms of ocular dominance plasticity in visual cortex. Philos Trans R Soc Lond Biol Sci 2009;364:357–367. [PubMed: 18977732]

Simons DJ, Carvell GE. Thalamocortical responses transformation in the rat vibrissa/barrel system. J Neurophysiol 1989;61:311–330. [PubMed: 2918357]

Steinert JR, Postlethwaite M, Jordan MD, Chernova T, Robinson SW, Forsythe ID. NMDA-R-mediated EPSCs are maintained and accelerate in time course during maturation of mouse and rat auditory system. J Physiol (Lond) 2010;588:447–463. [PubMed: 20008465]

Townsend M, Yoshii A, Mishina M, Constantine-Paton M. Developmental loss of miniature N-methyl-D-aspartate receptor currents in NR2A knockout mice. Proc Natl Acad Sci USA 2003;100:1340–1345. [PubMed: 12552130]

Tse Y-C, Lai C-H, Lai S-K, Liu J-X, Yung Ken KL, Shum Daisy KY, Chan Y-S. Developmental expression of NMDA and AMPA receptor subunits in vestibular nuclear neurons that encode gravity-related horizontal orientations. J Comp Neurol 2008;58:343–364. [PubMed: 18335497]

Turman JE, Lee OK, Chandler SH. Differential NR2A and NR2B expression between trigeminal neurons during early postnatal development. Synapse 2002;44:76–85. [PubMed: 11891879]

Verdoorn TA, Burnashev N, Monyer H, Seeburg PH, Sakmann B. Structural determinants of ion flow through recombinant glutamate receptor channels. Science 1991;252:1715–1718. [PubMed: 1710829]

Vicini S, Wang JF, Li JH, Zhu WJ, Wang YH, Luo JH, Wolfe BB, Grayson DR. Functional and pharmacological differences between recombinant N-methyl-D-aspartate receptors. J Neurophysiol 1998;79:555–566. [PubMed: 9463421]

Waite PME, Ho SM, Henderson TA. Afferent ingrowth and onset of activity in the rat trigeminal nucleus. Eur J Neurosci 2000;12:2781–2792. [PubMed: 10971620]

Wenthold RJ, Prybylowski K, Standley S, Sans N, Petralia RS. Trafficking of NMDA receptors. Annu Rev Pharmacol Toxicol 2003;43:335–358. [PubMed: 12540744]

Williams K. Ifenprodil discriminates subtypes of the N-methyl-d-aspartate receptor: selectivity and mechanisms at recombinant heteromeric receptors. Mol Pharmacol 1993;44:851–859. [PubMed: 7901753]

Xing G-G, Wang R, Yang B, Zhang D. Postnatal switching of NMDA receptor subunits from NR2B to NR2A in rat facial motor neurons. Eur J Neurosci 2006;24:2987–2992. [PubMed: 17156360]

Yashiro K, Philpot BD. Regulation of NMDA receptor subunit expression and its implications for LTD, LTP, and metaplasticity. Neuropharmacology 2008;55:1081–1094. [PubMed: 18755202]

Ye G-L, Yi S, Gamkrelidz G, Pasternak JF, Trommer BL. AMPA and NMDA receptor-mediated currents in developing dentate gyrus granule cells. Dev Brain Res 2005;155:26–32. [PubMed: 15763272]

Zhou M. Plasticity of NMDA receptor NR2B subunit in memory and chronic pain. Mol Brain 2009;2:4. [PubMed: 19192303]

Zundert B, Yoshii A, Constantine-Paton M. Receptor compartmentalization and trafficking at glutamate synapses: a developmental proposal. Trends in Neuroscience 2004;22:428–37.

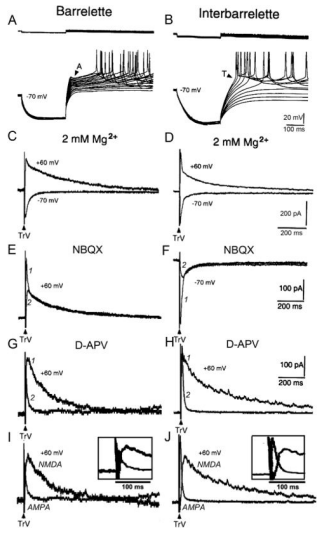

Fig. 1.

Excitatory responses are mediated by both AMPA and NMDA receptors in barrelette and interbarrelette cells. (A) Barrelette cells are characterized by a transient K^+ conductance (I_A) that delays the generation of Na^+ spikes upon membrane depolarization. (B) Interbarrelette cells are distinguished by a low threshold T-type Ca^{2+} conductance (I_T) that results in a triangular depolarization. (C, D) EPSCs contain an early fast declining and late slowly declining components. With the presence of Mg^{2+} (2 mM) in ACSF and GABAergic antagonist, the late component of the EPSC at −70 mV is much smaller in amplitude than that at +60 mV, suggesting the EPSCs are mediated by both AMPA and NMDA receptors. Each record is an average of 10 traces in this and subsequent figures.

(E, F) Both in barrelette and interbarrelette cells, the early component of EPSCs is blocked by 10 μM NBQX, an antagonist of AMPA receptors (*1 vs. 2 traces*). Note that even in the presence of 2 mM Mg^{2+}, a considerable amount of NMDA-EPSC remained at −70 mV (interbarrelette cell *trace 2*). (G, H) The late component of EPSCs is blocked by 100 μM D-APV, an NMDAR antagonist (*1 vs. 2 traces*). (I, J) Superimposed D-APV-sensitive NMDA-EPSCs and pharmacologically isolated AMPA-EPSCs indicate that the peaks of AMPA-EPSC and NMDA-EPSC separate from each other (insets show expanded traces with very little overlap of the peaks of EPSCs).

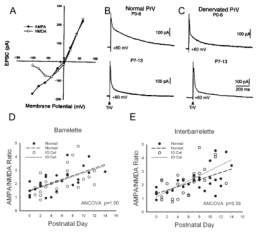

Fig. 2.

Developmental increase in AMPA/NMDA ratio in the PrV. (A) An example of measurement of compound EPSCs at different holding potentials. The amplitude at 8 ms shows an AMPA-like linear voltage-dependency. The amplitude at 30 ms displays a typical NMDA voltage-dependency. (B) Example records illustrating the increase in AMPA/NMDA ratio at the second postnatal week in the normal PrV (upper vs. lower traces). (C) Example records showing the developmental increase in AMPA/NMDA ratio in the denervated PrV (upper vs. lower traces). (D) Linear correlation and regression between the AMPA/NMDA ratio and postnatal ages in the normal (closed circles, dashed line) and denervated barrelette neurons (open circles, dotted line). The analysis of covariance (ANCOVA) shows the slopes and intercepts of regression lines are the same (p=1.00). (E) Linear correlation and regression between the AMPA/NMDA ratio and postnatal ages in the normal (closed circles, dashed line) and denervated interbarrelette neurons (open circles, dotted line). The analysis of covariance (ANCOVA) shows the slopes and intercepts of regression lines are similar (p=0.58).

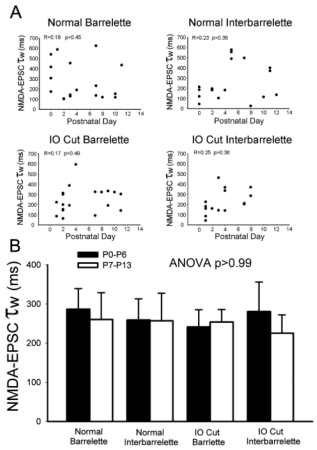

Fig. 3.

Subunit composition of NMDARs remains constant in developing and denervated PrV. (A) Plots of NMDA-EPSC τ_w against postnatal ages in the normal or denervated barrelette and interbarrelette neurons. There is no (linear or non-linear) correlation suggesting that the NMDAR subunit composition remains constant during postnatal development. (B) The averaged τ_w of NMDA-EPSCs in the first postnatal week (black bars) does not significantly differ from that of the second week (white bars) in the normal or denervated barrelette and interbarrelette neurons. There is no significant difference among the four groups (ANOVA test p=0.99). Therefore, the NR2A, NR2B subunits are not developmentally regulated and do not depend on sensory activity from the whiskers.

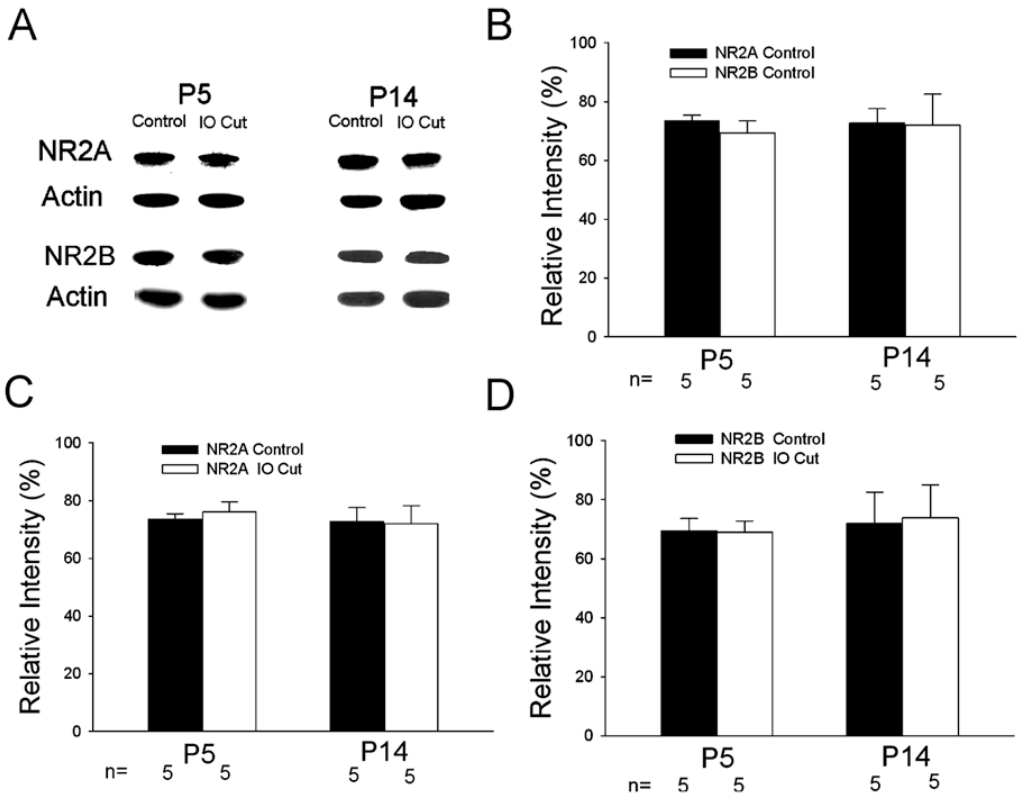

Fig. 4.

Assessment of NR2A and NR2B expression in the PrV by Western blot analysis. (A) NR2A and NR2B protein levels at P5 and P14 in the developing and denervated PrV. (B) NR2A and NR2B expression on the normal side of the PrV at different ages. The intensity measurements of NR2A and NR2B were normalized to actin levels and expressed as relative intensity. The averaged relative intensity is expressed by mean±S.E.M. In the normal PrV (control), NR2A and NR2B expressions are about the same at P5 and P14 (ANOVA test $p=0.97$); suggesting that there is no developmental change in NR2A and NR2B levels and no significant difference ($n=5$, $p=0.97$) between NR2A and NR2B expression. (C) Comparison of NR2A expression on the normal and denervated sides at different ages. ANOVA test ($p=0.75$) shows no significant difference between both sides. (D) Comparison of NR2B expression on the normal and denervated sides of the PrV at different ages. ANOVA test ($p=0.97$) shows no significant difference between both sides.